J|A|C|S
ARTICLES
Published on Web 05/06/2006

Antibiofouling Polymer-Coated Superparamagnetic Iron Oxide Nanoparticles as Potential Magnetic Resonance Contrast Agents for in Vivo Cancer Imaging

Haerim Lee,[†] Eunhye Lee,[†] Do Kyung Kim,[‡] Nam Kyu Jang,[§] Yong Yeon Jeong,*[,§] and Sangyong Jon*[,†]

Contribution from the Department of Life Science, Gwangju Institute of Science and Technology (GIST), 1 Oryoung-dong, Buk-gu, Gwangju 500-712, Republic of Korea, Institute for Science and Technology in Medicine, Keele University, Thronburrow Drive, Hartshill, Stoke-on-Trent, ST4 7QB United Kingdom, and Department of Diagnostic Radiology, Chonnam National University Medical School, Gwangju 501-746, Republic of Korea

Received March 6, 2006; E-mail: syjon@gist.ac.kr; yjeong@chonnam.ac.kr

Abstract: We report the fabrication and characterization of antifouling polymer-coated magnetic nanoparticles as nanoprobes for magnetic resonance (MR) contrast agents. Magnetite superparamagnetic iron oxide nanoparticles (SPION) were coated with the protein- or cell-resistant polymer, poly(TMSMA-*r*-PEGMA), to generate stable, protein-resistant MR probes. Coated magnetic nanoparticles synthesized using two different preparation methods (in situ and stepwise, respectively) were both well dispersed in PBS buffer at a variety of pH conditions (pH 1−10). In addition, dynamic light scattering data revealed that their sizes were not altered even after 24 h of incubation in 10% serum containing cell culture medium, indicative of a lack of protein adsorption on their surfaces. When the antibiofouling polymer-coated SPION were incubated with macrophage cells, uptake was significantly lower in comparison to that of the popular contrast agent, Feridex I.V., suggesting that the polymer-coated SPION can be long-circulated in plasma by escaping from uptake by the reticular endothelial system (RES) such as macrophages. Indeed, when the coated SPION were administered to tumor xenograft mice by intravenous injection, the tumor could be detected in T2-weighted MR images within 1 h as a result of the accumulation of the nanomagnets within the tumor site. Although the poly(TMSMA-*r*-PEGMA)-coated SPION do not have any targeting ligands on their surface, they are potentially useful for cancer diagnosis in vivo.

Introduction

Superparamagnetic iron oxide nanoparticles (SPION) currently have a surge of interest as their potential has been demonstrated in biomedical applications such as magnetic resonance imaging (MRI),[1−8] drug delivery,[9,10] and therapy (hyperthermia).[11,12] SPION may potentially provide higher contrast enhancement in MRI than conventional paramagnetic Gd-based contrast agents[13−15] due to their superparamagnetic property.[16,17] However, the direct use of SPION as in vivo MRI contrast agents results in biofouling of the particles in blood plasma and formation of aggregates that are quickly sequestered by cells of the reticular endothelial system (RES) such as macrophages.[18,19] Furthermore, aggregated SPION reduce the intrinsic superparamagnetic properties.[11] Such fast clearance of SPION is known to be triggered by the "opsonization" process,[20] nonspecific adsorption of plasma proteins onto the particles' surface, which occurs more efficiently due to its innate high surface-to-volume ratio as well as attractive forces between the nanomagnetites.[11,21] Therefore, it is essential to engineer the surface of the SPION to minimize biofouling and aggregation

[†] Gwangju Institute of Science and Technology.
[‡] Keele University.
[§] Chonnam National University Medical School.

(1) Baghi, M.; Mack, M. G.; Hambek, M.; Rieger, J.; Vogl, T.; Gstoettner, W.; Knecht, R. *Anticancer Res.* **2005**, *25*, 3665−3670.
(2) Martina, M. S.; Fortin, J. P.; Menager, C.; Clement, O.; Barratt, G.; Grabielle-Madelmont, C.; Gazeau, F.; Cabuil, V.; Lesieur, S. *J. Am. Chem. Soc.* **2005**, *127*, 10676−10685.
(3) Blasberg, R. G. *Mol. Cancer Ther.* **2003**, *2*, 335−343.
(4) Artemov, D. *J. Cell. Biochem.* **2003**, *90*, 518−524.
(5) Schmitz, S. A. *RoeFo, Fortschr. Geb. Roentgenstr. Nuklearmed.* **2003**, *175*, 469−476.
(6) Kroft, L. J.; de Roos, A. *J. Magn. Reson. Imaging* **1999**, *10*, 395−403.
(7) Bonnemain, B. *J. Drug Targeting* **1998**, *6*, 167−174.
(8) Bellin, M. F.; Beigelman, C.; Precetti-Morel, S. *Eur. J. Radiol.* **2000**, *34*, 257−264.
(9) Kohler, N.; Sun, C.; Wang, J.; Zhang, M. *Langmuir* **2005**, *21*, 8858−8864.
(10) Gupta, A. K.; Curtis, A. S. *J. Mater. Sci.: Mater. Med.* **2004**, *15*, 493−496.
(11) Gupta, A. K.; Gupta, M. *Biomaterials* **2005**, *26*, 3995−4021.
(12) Ito, A.; Kuga, Y.; Honda, H.; Kikkawa, H.; Horiuchi, A.; Watanabe, Y.; Kobayashi, T. *Cancer Lett.* **2004**, *212*, 167−175.
(13) Aime, S.; Cabella, C.; Colombatto, S.; Geninatti Crich, S.; Gianolio, E.; Maggioni, F. *J. Magn. Reson. Imaging* **2002**, *16*, 394−406.
(14) Arbab, A. S.; Bashaw, L. A.; Miller, B. R.; Jordan, E. K.; Lewis, B. K.; Kalish, H.; Frank, J. A. *Radiology* **2003**, *229*, 838−846.
(15) Kaim, A. H.; Wischer, T.; O'Reilly, T.; Jundt, G.; Frohlich, J.; von Schulthess, G. K.; Allegrini, P. R. *Radiology* **2002**, *225*, 808−814.
(16) Jung, C. W.; Jacobs, P. *Magn. Reson. Imaging* **1995**, *13*, 661−674.
(17) Benderbous, S.; Corot, C.; Jacobs, P.; Bonnemain, B. *Acad. Radiol.* **1996**, *3* (Suppl 2), S292−294.
(18) Raynal, I.; Prigent, P.; Peyramaure, S.; Najid, A.; Rebuzzi, C.; Corot, C. *Invest. Radiol.* **2004**, *39*, 56−63.
(19) Rogers, W. J.; Basu, P. *Atherosclerosis* **2005**, *178*, 67−73.
(20) Moghimi, S. M.; Hunter, A. C.; Murray, J. C. *Pharmacol. Rev.* **2001**, *53*, 283−318.
(21) Jung, C. W. *Magn. Reson. Imaging* **1995**, *13*, 675−691.

of the particles in physiological conditions (i.e., high salt and protein concentrations) for long periods.[22−24]

Several synthetic and natural polymers have been employed to modify the surface of the SPION to enhance their function in vivo.[11] These polymers include dextran,[25,26] poly(ethylene glycol)s (PEG),[10,23,27] and poly(vinylpyrrolidone) (PVP),[28] all of which are known to be biocompatible and result in a long blood-circulating SPION. Monocrystalline iron oxide nanoparticles (MION) and cross-linked iron oxide nanoparticles (CLIO) are typical examples of dextran-coated SPION having a magnetite core (Fe_3O_4 in chemical composition) and have been widely used for in vivo as well as in vitro MRI.[29−33] Of synthetic polymers, PEG coating on SPION has been known to improve biocompatibility and blood circulation times.[10,20,34] However, since PEG coating in the previous systems has been achieved through noncovalent interactions, there is a potential concern about the stability of the PEG coat in physiological medium.[23,35] In addition, to our knowledge, none of the previous PEG-coated SPION have been demonstrated as MR contrast agents for in vivo cancer imaging.

We have previously developed an antibiofouling copolymeric system comprising a "surface anchoring moiety" (silane group) and a "protein-resistant moiety" (PEG), denoted as poly(TMSMA-*r*-PEGMA), which is a random copolymer synthesized from (trimethoxysilyl)propyl methacrylate and PEG methacrylate.[36] With the use of the PEG−silane copolymer system, protein- and cell-resistant surfaces could be generated on Si/SiO_2 substrates by forming polymeric monolayers (PMs) via multiple covalent bonds.[36−40] In this study we examine the feasibility of this polymeric system as an antifouling coating material for magnetic nanoparticles, especially magnetite SPION. Specifically, we analyze (1) the synthesis and characterization of the poly(TMSMA-*r*-PEGMA)-coated SPION, denoted as poly(TMSMA-*r*-PEGMA)@SPION, and (2) their efficacy as cancer in vivo imaging agents using conventional clinical 1.5 T MRI. We have synthesized two types of poly(TMSMA-*r*-PEGMA)@SPION under different preparation conditions and compared in vitro and in vivo the properties of each SPION as an MR contrast agent.

Experimental Section

Materials. 3-(Trimethoxysilyl)propyl methacrylate (TMSMA, 98%), poly(ethylene glycol) methyl ether methacrylate (PEGMA, average M_n = ca. 475), tetrahydrofuran (THF, anhydrous, 99.9%, inhibitor-free), 2,2′-azobisisobutyronitrile (AIBN, 98%), ferric chloride hexahydrate ($FeCl_3 \cdot 6H_2O$), ferrous chloride tetrahydrate ($FeCl_2 \cdot 4H_2O$), dimethyl sulfoxide (DMSO), potassium ferrocyanide(II) trihydrate ($K_4Fe(CN)_6 \cdot 3H_2O$), nuclear fast red solution, MTT solution, and PFA (paraformaldehyde) were purchased from Sigma-Aldrich Chemical Co. (St. Louis, MO). Ammonium hydroxide solution (∼28% in water) was purchased from Fluka (Buchs, Switzerland). Feridex I.V. was purchased from Advanced Magnetics Inc. (Cambridge, MA). Other organic solvents were used as received. A rare-earth magnet (N35 grade, cylinder type, dimensions: 5 cm in diameter, 2 cm in height) was purchased by Daehan-magnet Co. (Seoul, South Korea).

Measurements. The saturation magnetization (M_s) value was measured by a magnetic property measurement system (MPMS) of Quantum Design at 300 K. The applied magnetic field was varied from 10 000 Oe to −10 000 Oe. The M_s in emu/g was normalized with the wt % of magnetite derived from thermogravimetric analysis (TGA) to obtain emu/g iron. The hydrodynamic particle sizes of IS- and SW-SPION were measured using an ELS 8000 from Otsuka Electronics Korea (Seoul, South Korea), where "IS" and "SW" denote "in situ" and "stepwise", respectively. The size and dispersion quality of both IS- and SW-SPION were investigated with transmission electron microscopy (TEM) using a Philips TECNAI F20 at 200 kV. For TEM sample preparation, IS- and SW-SPION were diluted and deposited on a carbon-coated copper grid and allowed to air-dry.

Synthesis of Poly(TMSMA-*r*-PEGMA)-Coated SPION. For IS-SPION synthesis, the formation of the magnetite core and the polymer coating takes place simultaneously. For the SW-SPION synthesis, magnetite cores are formed in the absence of polymer, after which the resulting magnetite particles are coated with polymer.

A. IS-SPION. Poly(TMSMA-*r*-PEGMA)[36] (250 mg), $FeCl_3 \cdot 6H_2O$ (0.5 g, 1.85 mmol), and $FeCl_2 \cdot 4H_2O$ (0.184 g, 0.925 mmol) were dissolved in deoxygenated distilled water (30 mL) using N_2 streaming for 20 min. To this solution was added 7.5 mL of NH_4OH (∼28% in water) while stirring vigorously in a N_2 atmosphere. At this time, the pH of the mixture changed from around 1.8 to above 10.5, coincidently with a color change to dark black, indicative of formation of iron oxide particles. To remove the remaining unreacted polymer in solution, an external magnetic field (M_{ext}) was applied to the solution using a rare-earth magnet. Within minutes all the black particles sank down toward the magnet, and the supernatant was discarded. The black precipitate was stirred gently in 30 mL of distilled water to redisperse it, and M_{ext} was applied again to remove the supernatant. Washing was repeated twice more, and finally, the remaining particles were sonicated at 200 W in 30 mL of distilled water for 15 min using an ultrasonic processor (VCX-500) of SONICS & MATERIALS INC. Afterward, M_{ext} was applied overnight to precipitate aggregated particles. Most of the particles existed in the supernatant, while a small portion of particles sank down. Only the supernatant was collected with care. Note: the collected supernatant layer was then heated at 80 °C for 1 h to achieve cross-linking between entangled polymer chains on the particle surface. The resulting cross-linked poly(TMSMA-*r*-PEGMA)@SPION were centrifuged at 6000 rpm for 10 min and subsequently at 10 000 rpm for 10 min to further remove very small aggregates that might exist in the solution. The resulting IS-SPION were stored at 4 °C before use.

B. SW-SPION. $FeCl_3 \cdot 6H_2O$ (0.5 g, 1.85 mmol) and $FeCl_2 \cdot 4H_2O$ (0.184 g, 0.925 mmol) were dissolved in deoxygenated distilled water

(22) Shieh, D. B.; Cheng, F. Y.; Su, C. H.; Yeh, C. S.; Wu, M. T.; Wu, Y. N.; Tsai, C. Y.; Wu, C. L.; Chen, D. H.; Chou, C. H. *Biomaterials* **2005**, *26*, 7183−7191.
(23) Kohler, N.; Fryxell, G. E.; Zhang, M. *J. Am. Chem. Soc.* **2004**, *126*, 7206−7211.
(24) Mikhaylova, M.; Kim do, K.; Bobrysheva, N.; Osmolowsky, M.; Semenov, V.; Tsakalakos, T.; Muhammed, M. *Langmuir* **2004**, *20*, 2472−2477.
(25) Kaufman, C. L.; Williams, M.; Ryle, L. M.; Smith, T. L.; Tanner, M.; Ho, C. *Transplantation* **2003**, *76*, 1043−1046.
(26) Berry, C. C.; Wells, S.; Charles, S.; Aitchison, G.; Curtis, A. S. *Biomaterials* **2004**, *25*, 5405−5413.
(27) Zhang, Y.; Kohler, N.; Zhang, M. *Biomaterials* **2002**, *23*, 1553−1561.
(28) D'Souza, A. J.; Schowen, R. L.; Topp, E. M. *J. Controlled Release* **2004**, *94*, 91−100.
(29) Choi, H.; Choi, S. R.; Zhou, R.; Kung, H. F.; Chen, I. W. *Acad. Radiol.* **2004**, *11*, 996−1004.
(30) Josephson, L.; Tung, C. H.; Moore, A.; Weissleder, R. *Bioconjugate Chem.* **1999**, *10*, 186−191.
(31) Hogemann, D.; Josephson, L.; Weissleder, R.; Basilion, J. P. *Bioconjugate Chem.* **2000**, *11*, 941−946.
(32) Lewin, M.; Carlesso, N.; Tung, C. H.; Tang, X. W.; Cory, D.; Scadden, D. T.; Weissleder, R. *Nat. Biotechnol.* **2000**, *18*, 410−414.
(33) Josephson, L.; Kircher, M. F.; Mahmood, U.; Tang, Y.; Weissleder, R. *Bioconjugate Chem.* **2002**, *13*, 554−560.
(34) Tiefenauer, L. X.; Tschirky, A.; Kuhne, G.; Andres, R. Y. *Magn. Reson. Imaging* **1996**, *14*, 391−402.
(35) Gellissen, J.; Axmann, C.; Prescher, A.; Bohndorf, K.; Lodemann, K. P. *Magn. Reson. Imaging* **1999**, *17*, 557−567.
(36) Jon, S.; Seong, J.; Khademhosseini, A.; Tran, T. T.; Laibinis, P. E.; Langer, R. *Langmuir* **2003**, *19*, 9889−9893.
(37) Khademhosseini, A.; Jon, S.; Suh, K. Y.; Tran, T. T.; Eng, G.; Yeh, J.; Seong, J.; Langer, R. *Adv. Mater.* **2003**, *15*, 1995−2000.
(38) Khademhosseini, A.; Suh, K. Y.; Jon, S.; Eng, G.; Yeh, J.; Chen, G. J.; Langer, R. *Anal. Chem.* **2004**, *76*, 3675−3681.
(39) Khademhosseini, A.; Yeh, J.; Jon, S.; Eng, G.; Suh, K. Y.; Burdick, J. A.; Langer, R. *Lab-on-a-Chip* **2004**, *4*, 425−430.
(40) Suh, K. Y.; Jon, S. *Langmuir* **2005**, *21*, 6836−6841.

(30 mL) using N_2 streaming for 20 min. To this solution was added 7.5 mL of NH_4OH (~28% in water) while stirring vigorously in a N_2 atmosphere. To the black precipitate was added 30 mL of distilled water. The solution was stirred gently to redisperse it, and M_{ext} was applied to remove the supernatant. After discarding the supernatant, 250 mg of poly(TMSMA-*r*-PEGMA) in 30 mL of distilled water was added and stirred. Washing and subsequent steps were the same as for IS-SPION.

Cell Culture and Preparation. Lewis lung carcinoma (LLC) cell line (American Type Culture Collection, Manassas, VA) and macrophage cell line RAW 264.7 (Korean Cell Line Bank, Seoul, South Korea) were maintained as an adherent culture and grown as a monolayer in a humidified incubator (95% air; 5% CO_2) at 37 °C in a Petri dish (Nunc) containing DMEM (GIBCO) supplemented with 10% (v/v) heat-inactivated fetal bovine serum (FBS, GIBCO), 100 IU/mL penicillin (GIBCO), and 100 IU/mL streptomycin (GIBCO). For experiments, each cell was detached mechanically and adjusted to the required concentration of viable cells, by counting in a hemocytometer in the presence of trypan blue.

In Vitro Cell Cytotoxicity Analysis. The LLC cell line was used to measure the in vitro cell cytotoxicity of IS- and SW-SPION. An amount of 10^5 cells of LLC was plated in each well of a 96-well plate 24 h before washing with PBS (pH 7.4) and adding either IS- or SW-SPION at the desired concentrations (from 1 to 100 μg iron per well). After 12 h of incubation, the supernatant was removed and cells were washed three times with PBS (pH 7.4). Cell viability was then estimated using the MTT conversion test. Briefly, 100 μL of MTT solution was added to each well. After incubation for 4 h, each well was treated with 100 μL of DMSO with pipetting for 3 to ~5 min. Absorption at 570 nm was measured on a plate reader. Each result was the average of four wells, and 100% viability was determined from untreated cells.

Nanoparticle Uptake by Macrophages. Gelatin-coated coverslips were placed in 35 Π dishes (SPL Lifesciences, South Korea) containing DMEM. RAW 264.7 macrophages were seeded onto each coverslip with 10^5 cells/coverslip. After incubation for 20 h, IS-SPION, SW-SPION, and Feridex I.V. diluted in DMEM were added to a 24-well plate in a final concentration of 0.6 mg iron/well or 0.3 mg iron/well. After 2 h, each well was washed with PBS, treated with 0.5 mL of 4% PFA solution for 10 min to fix the cells, and then washed with PBS. Cells were stained with Prussian blue. To each well was added a 0.5 mL of a 2:1 mixture of 2% potassium ferrocyanide(II) trihydrate and 2% HCl solution, and cells were incubated for 20 min in a 37 °C water bath, after which each well was washed three times with PBS. Each coverslip was placed on a slide and treated with PermaFluor Mountant Medium mounting media and then dried for 1 day. The Prussian blue staining result was assessed by a light microscope.

In Vivo MR Imaging. For all animals, MR images were taken prior to injection of both SPION and at appropriate time points of postinjection. Mice were anesthetized for imaging with the use of a general inhalation anesthesia (1.5% isoflurane in a 1:2 mixture of O_2/N_2). The polymer-coated SPION were injected intravenously through the tail vein. MR imaging was performed with a 1.5 T imager (GE Signa Exite Twin-speed, GE Health Care, Milwaukee, WI) using an animal coil (4.3 cm Quadrature volume coil, Nova Medical System, Wilmington, DE). For MR imaging of mice, T2-weighted fast-spin−echo (repetition time ms/echo time ms of 4200/102, flip angle of 90°, echo train length of 10, 5 cm field of view, 2 mm section thickness, 0.2 mm intersection gap, 256 × 160 matrix) and T1-weighted spoiled gradient echo (185/minimum, 60° flip angle, 2 mm section thickness, 0.2 mm intersection gap, 256 × 160 matrix) sequences were performed.

The quantitative analysis was performed by one radiologist for all MR imaging. The signal intensity (SI) was measured in defined regions of interest (ROI), which were in comparable locations within the tumor center. In addition, the SI in ROI of back muscle adjacent to the tumor was measured. The size of the ROI was chosen as two-thirds the maximum diameter of the tumor. Relative signal enhancement was calculated by using SI measurements before (SI pre) and after (SI post) injection of the contrast agents by using the formula [(SI post − SI pre)/SI pre] × 100, where SI pre is the lesion signal intensity on the pre-enhanced scan (control) and SI post is the lesion signal intensity on the postenhanced scan at 1, 2.5, and 4 h.

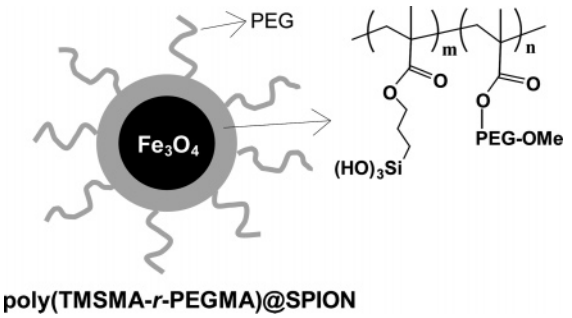

Figure 1. Schematic diagram of the polymer-coated SPION and chemical structure of the PEG−silane copolymer, poly(TMSMA-*r*-PEGMA).

Results and Discussion

Surface modifications of SPION with biocompatible polymers are potentially beneficial to prepare MR contrast agents for in vivo applications.[10,34] In particular, an antifouling or protein-resistant surface is required for the nanoparticles to accumulate in tumors by the enhanced permeability and retention (EPR) effect[41,42] during systemic circulation. Otherwise nanoparticles are quickly cleared by RES due to increased particle size as a result of aggregation.[18,19,43] According to a general synthetic protocol for polymer-coated SPION, polymer coating takes place simultaneously while the iron oxide core is formed in aqueous alkali solution (pH > 10).[29,44] On the other hand, polymer coating can be done separately once the iron oxide core is formed and separated. In this paper, we denoted the former as the "in situ" (IS) and the latter as the "stepwise" (SW) method.

Since the presence of polymer can interfere with the nucleation step of iron oxide formation, the "IS" method usually results in smaller sizes as well as lower magnetization of SPION than the equivalent prepared in the absence of polymers.[2,10] In contrast, such interference is not involved in the "SW" method because the polymer coating process occurs onto the existing magnetite. Based on this fact, we prepared the poly(TMSMA-*r*-PEGMA)-coated magnetites using both "IS" and "SW" methods, which are denoted as "IS-SPION" and "SW-SPION", respectively. While IS-SPION were synthesized by adding NH_4-OH solution to a mixture of Fe^{2+}, Fe^{3+}, and poly(TMSMA-*r*-PEGMA) in water, SW-SPION were prepared by adding aqueous poly(TMSMA-*r*-PEGMA) solution to the as-synthesized magnetite. The polymer contains multiple PEG and silane groups per polymer and is proven to render the materials' surfaces highly protein-resistant by forming PMs via multiple covalent bonds (Figure 1).[36−40] Upon polymer coating the hydrophilic PEG is likely to be present at the outermost surface of the SPION, and the hydrolyzed silane part would form multiple covalent bonds at the polymer−magnetite interface, while a majority of the polymer chains are entangled to each

(41) Maeda, H.; Matsumura, Y. *Crit. Rev. Ther. Drug Carrier Syst.* **1989**, *6*, 193−210.
(42) Matsumura, Y.; Maeda, H. *Cancer Res.* **1986**, *46*, 6387−6392.
(43) Herrwerth, S.; Eck, W.; Reinhardt, S.; Grunze, M. *J. Am. Chem. Soc.* **2003**, *125*, 9359−9366.
(44) Funovics, M. A.; Kapeller, B.; Hoeller, C.; Su, H. S.; Kunstfeld, R.; Puig, S.; Macfelda, K. *Magn. Reson. Imaging* **2004**, *22*, 843−850.

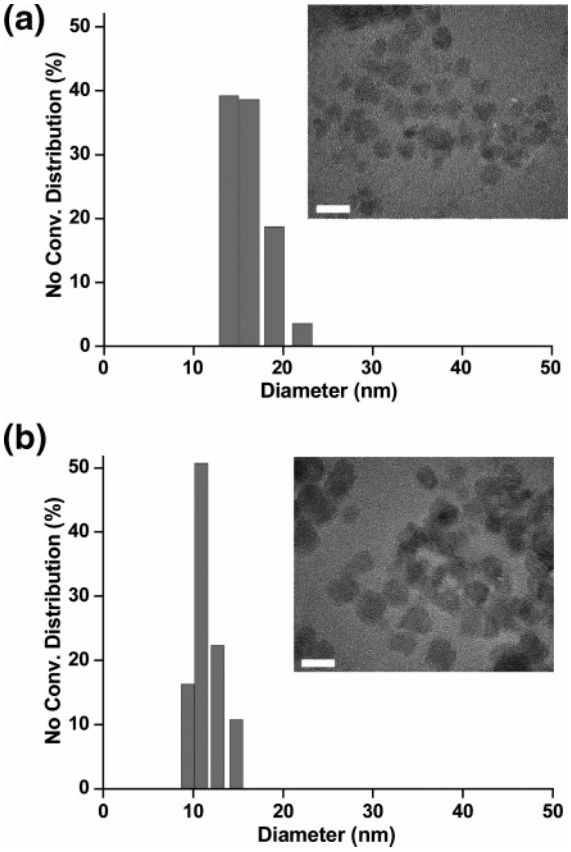

Figure 2. Hydrodynamic size distribution graphs along with TEM images of (a) IS-SPION and (b) SW-SPION. The scale bar in the TEM images denotes 10 nm.

other to form multilayers in between. The poly(TMSMA-*r*-PEGMA) coating layers were further hardened by cross-linking reactions between silane groups of the polymer chains during the heating process, which is one of the favorable characteristics of this polymer system in making stable poly(TMSMA-*r*-PEGMA) coatings. The schematic representation of the poly(TMSMA-*r*-PEGMA)@SPION is shown in Figure 1. In this study we examine (1) the feasibility of the poly(TMSMA-*r*-PEGMA)@SPION as MR contrast agents and (2) which preparation method would result in enhanced functional properties of the resulting contrast agent.

To examine the formation of the poly(TMSMA-*r*-PEGMA)@SPION, particle size, crystallinity, and magnetization measurements were performed. FT-IR spectra of the poly(TMSMA-*r*-PEGMA)@SPION confirmed the existence of the polymer in the purified nanoparticles, showing characteristic peaks of the poly(TMSMA-*r*-PEGMA) around 1720, 1105, and 627 cm^{-1} that correspond to stretching bands of C═O, C−O, and Si−O, respectively (Figure S1 in the Supporting Information). TGA revealed that the weight percentage of the polymer in each type of SPION was 45% for IS-SPION and 30% for SW-SPION, respectively (Figure S2 in the Supporting Information).

Dynamic light scattering (DLS) measurements revealed that both IS- and SW-SPION showed relatively narrow size distributions with mean sizes of 16.0 ± 2.2 nm and 12.3 ± 1.2 nm, respectively (Figure 2), which are much smaller than those of the conventional dextran-coated SPION such as CLIO and

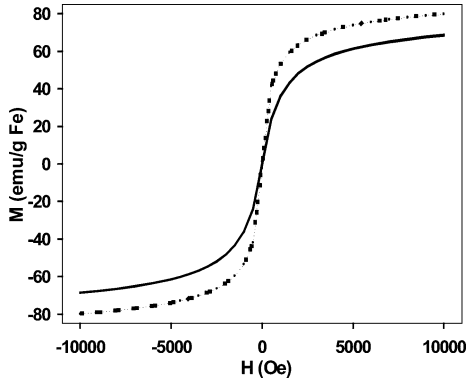

Figure 3. Variation of the magnetization of IS-SPION (solid line) and SW-SPION (dotted line) as a function of applied magnetic field.

MION.[45,46] Since DLS measurements provide information on the hydrodynamic particle size of whole clusters, including polymer coating layers and the magnetite core, TEM images were taken to measure the size of the iron oxide core only. As shown in the TEM images inserted in Figure 2, the core sizes of both IS- and SW-SPION were in the range of 4−8 nm, while the "SW" method led to the formation of slightly bigger iron oxide cores than the "IS" coating formation.[47] However, despite the bigger core size in the case of SW-SPION, their hydrodynamic diameter (∼12 nm) was smaller than that of the IS-SPION (∼16 nm). This suggests that much thinner polymer coating layers were formed than those on IS-SPION, evidenced by the TGA data (15 wt% less polymer exists for SW-SPION compared to that for IS-SPION).

Powder X-ray diffraction (XRD) analysis was taken to confirm the crystalline property of the poly(TMSMA-*r*-PEGMA)@SPION (Figure S3 in the Supporting Information). Both IS- and SW-SPION showed characteristic peaks that mainly correspond to magnetite (Fe_3O_4) when compared to those reported.[48] Since the polymer layers are formed onto the as-synthesized iron oxide in the case of SW-SPION, the magnetization property would not be altered after the coating process. In contrast, due to the interference of the polymer in the crystallization step of iron oxide nanoparticles, IS-SPION may have lower magnetization as compared to that of SW-SPION. When the magnetic moment was measured as a function of applied field at 300 K, both IS- and SW-SPION exhibited superparamagnetic behaviors showing high M_s of 65 and 80 emu/g Fe, respectively (Figure 3). As discussed, SW-SPION showed a larger magnetic moment than IS-SPION. It is noteworthy that the M_s value for the SW-SPION in this work is much larger than that of previously reported polymer-coated SPION which possess approximately 30−50 emu/g Fe,[48] thus providing a potential advantage for the "SW" process over the "IS" coating method.

To examine the stability of the SPION under physiological conditions for use as MR contrast agents,[22] we investigated the stability of SPION in PBS buffer solution and various pH

(45) Bulte, J. W.; Brooks, R. A.; Moskowitz, B. M.; Bryant, L. H., Jr.; Frank, J. A. *Acad. Radiol.* **1998**, *5* (Suppl 1), S137−140; discussion S145−146.
(46) Reimer, P.; Bader, A.; Weissleder, R. *J. Magn. Reson. Imaging* **1998**, *8*, 687−689.
(47) Jun, Y. W.; Huh, Y. M.; Choi, J. S.; Lee, J. H.; Song, H. T.; Kim, S.; Yoon, S.; Kim, K. S.; Shin, J. S.; Suh, J. S.; Cheon, J. *J. Am. Chem. Soc.* **2005**, *127*, 5732−5733.
(48) Cheng, F. Y.; Su, C. H.; Yang, Y. S.; Yeh, C. S.; Tsai, C. Y.; Wu, C. L.; Wu, M. T.; Shieh, D. B. *Biomaterials* **2005**, *26*, 729−738.

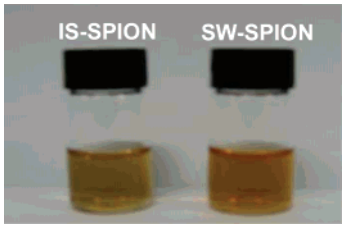

Figure 4. Photographs of IS-SPION and SW-SPION dispersed in phosphate-buffered saline (PBS, pH 7.4).

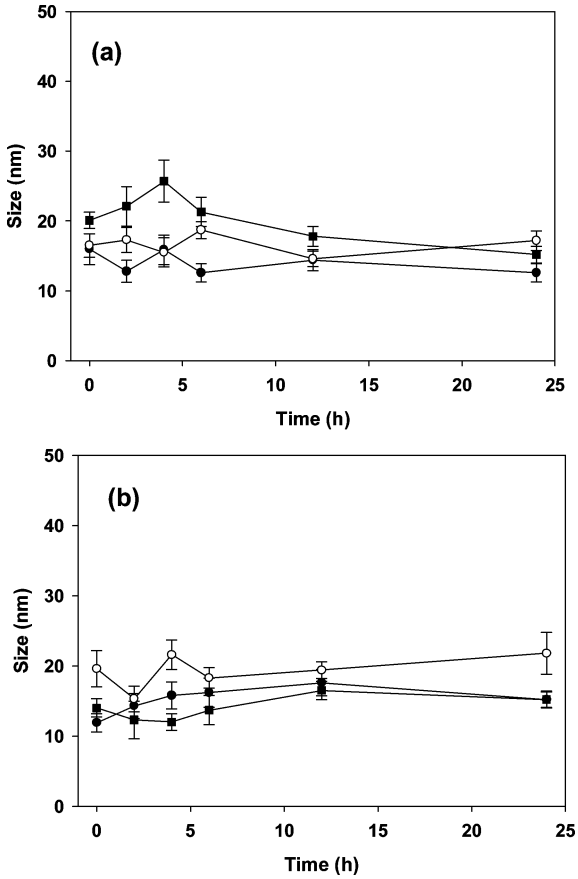

Figure 5. Hydrodynamic size distribution graphs of (a) IS-SPION and (b) SW-SPION measured as a function of time upon incubation in distilled water (closed circles), PBS (closed squares), and RPMI containing 10% FBS (open circles).

conditions. Both IS- and SW-SPION were fairy dispersed in PBS buffer solution (Figure 4) as well as in the pH range from 1 to 10 (Figure S4 in the Supporting Information) and furthermore did not show any aggregation for at least 1 month. In contrast, the naked SPION led to immediate precipitation or aggregation within 1 h (data not shown). This result implies that the poly(TMSMA-*r*-PEGMA) polymer system is able to not only passivate the surface charge of the SPION but also provide magnetic nanoparticles that remain suspended in aqueous media. To further verify the stability of the SPION under physiological conditions, the size changes of each type of SPION upon incubation in cell culture medium containing 10% FBS as simulated in vivo plasma were monitored. As shown in Figure 5a, the sizes of both IS- and SW-SPION were slightly altered by less than 5 nm after 24 h of incubation in RPMI medium containing 10% serum. In addition, we could not observe any aggregates upon incubation in distilled water and PBS buffer solution (Figure 5b). This is mainly attributed

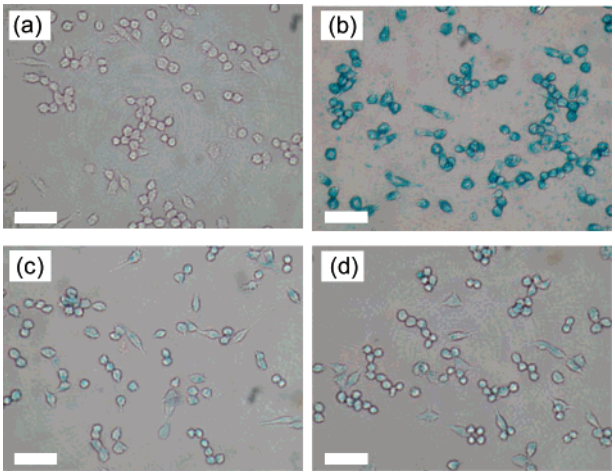

Figure 6. In vitro Prussian blue staining images of macrophage cell, RAW 264.7, after treatment with or without 0.6 mg Fe of each contrast agent: (a) control (without contrast agent), (b) Feridex, (c) IS-SPION, and (d) SW-SPION. The scale bar denotes 50 μm.

to the antibiofouling property of the poly(TMSMA-*r*-PEGMA) coating layers that play a key role in not only preventing the nanomagnets from aggregation, which is a result of nonspecific protein or salt adsorption, but also providing good water dispersibility by exposing hydrophilic PEG layers on the surface of the SPION.

Another key consideration for the in vivo use of SPION for cancer imaging is lower uptake of SPION by RES such as macrophages so that the magnetic nanoparticles can circulate long enough to be accumulated into the tumor by the EPR effect. To investigate this property in vitro cell uptake experiments were carried out using a macrophage cell line. The uptake of both IS- and SW-SPION by the macrophages was compared to that of Feridex I.V. which is currently used clinically for MRI and is known to be taken up by macrophages due to its size (>100 nm). To detect the presence of SPION in cells, Prussian blue staining was carried out after 2 h of incubation of each iron oxide nanoparticle with macrophages (Figure 6). As expected, most of cells were stained in blue as a result of high uptake in the case of Feridex I.V., whereas both IS- and SW-SPION showed significantly lower uptake. These results suggest that the antibiofouling coating layer with poly(TMSMA-*r*-PEGMA) in the present system drastically minimizes the recognition and phoagocytosis of the nanomagnets by macrophages.

MTT assay using the LLC cell line was performed to analyze the potential toxicity of the poly(TMSMA-*r*-PEGMA)@SPION. Figure 7 clearly indicates that both IS- and SW-SPION show no toxicity even at relatively high concentrations of the SPION. Since the amount of iron at the highest concentration (100 μg Fe/mL) far exceeds that of iron used in conventional SPION-based MR contrast agent for mice (1−20 mg/kg), the poly(TMSMA-*r*-PEGMA)@SPION herein could be used as safe MR contrast agents.

These results suggest that the IS- and SW-SPION in this study show high M_s, excellent dispersibility and long-term stability in physiological solution, low uptake by macrophages, and low cytotoxicity; thus, the antibiofouling poly(TMSMA-*r*-PEGMA)@SPION are good potential candidates as MR contrast agents for in vivo applications. On the basis of the in vitro data, the feasibility of the SPION for in vivo cancer diagnosis was

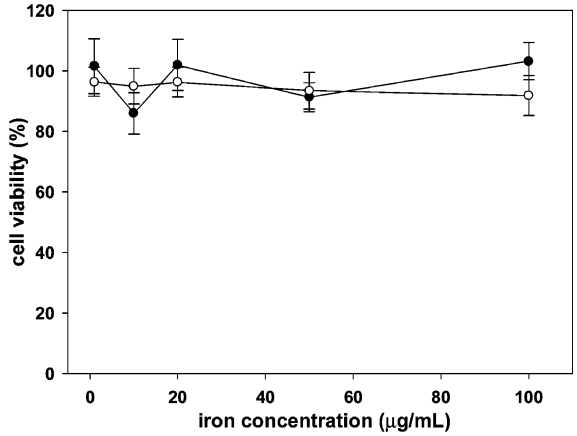

Figure 7. In vitro cell viability graphs of IS-SPION (closed circles) and SW-SPION (open circles) as a function of different iron concentrations of 1, 10, 20, 50, and 100 μg/10^5 cells by MTT assay.

examined by MRI. To date there have been only a few reports on direct imaging of cancers using polymer-coated SPION *parse* without attachment of specific targeting ligands on their surfaces, presumably because such SPION lacking the antibiofouling characteristic were easily taken up by RES. Since the poly(TMSMA-*r*-PEGMA)@SPION developed herein are fairly stable in a simulated plasma solution without agglutination and besides maintain their size far less than 20 nm, we postulated that the poly(TMSMA-*r*-PEGMA)@SPION upon systemic circulation could be accumulated in tumor sites by the EPR effect as a result of the presence of leaky vasculatures around tumors.[41,42]

Tumor-bearing mice were prepared by subcutaneous injection of the LLC cell line into the midback of mice, and then MR imaging of the mice was performed at scheduled time points after the intravenous injection of both IS- and SW-SPION in PBS buffer solution (15 and 13 mg/kg, respectively). Before injection of the SPION, tumors are seen as hyperintense areas in the T2-weighted MR images as indicated by white arrows (Figure 8). The relative SI on the T2-weighted image was calculated as described in the Experimental Section. At 1 h

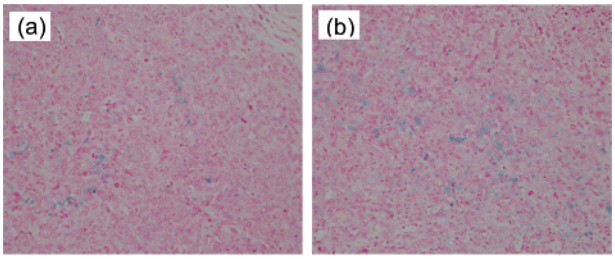

Figure 9. Ex vivo Prussian blue staining images of tumor tissues which were selected from mice at 4 h postinjection of (a) IS-SPION and (b) SW-SPION.

postinjection of the SPION, some areas of darkening on the T2-weighted MR images were observed in the tumor area with a T2 signal drop of 37% for IS-SPION and 42% for SW-SPION, respectively, indicative of the accumulation of detectable amounts of the SPION within the tumor. At 4 h postinjection slightly decreased yet significant (32%) of T2 signal drop relative to that of the control was observed in the case of SW-SPION, whereas the relative T2 signal drop of IS-SPION to that of the control was only 19%, indicating that IS-SPION were removed from the tumor much faster than SW-SPION. This suggests that cancer imaging is possible for up to 4 h with SW-SPION but not with IS-SPION due to their faster clearance. The higher accumulation of SW-SPION within the tumor as compared to that of IS-SPION may be attributed to their smaller size, resulting in the higher probability of penetration into the tumor. However, complete removal of both SPION from the tumor site was observed at 11 h postinjection (data not shown). Additionally, we observed some nanomagnet accumulation in kidneys within 1 h after the SPION injection. The nanoparticles were eventually cleared from the kidneys in a day.[49−51] This characteristic would be beneficial to develop safe, efficient MR contrast agents since potentially toxic iron oxides are eventually excreted from the body within a day while still efficiently diagnosing cancer in hours before renal clearance.

To further verify the existence of the SPION in the tumor area, Prussian blue staining was carried out.[52−55] As shown in Figure 9, parts of the tumor tissues were stained blue, indicative

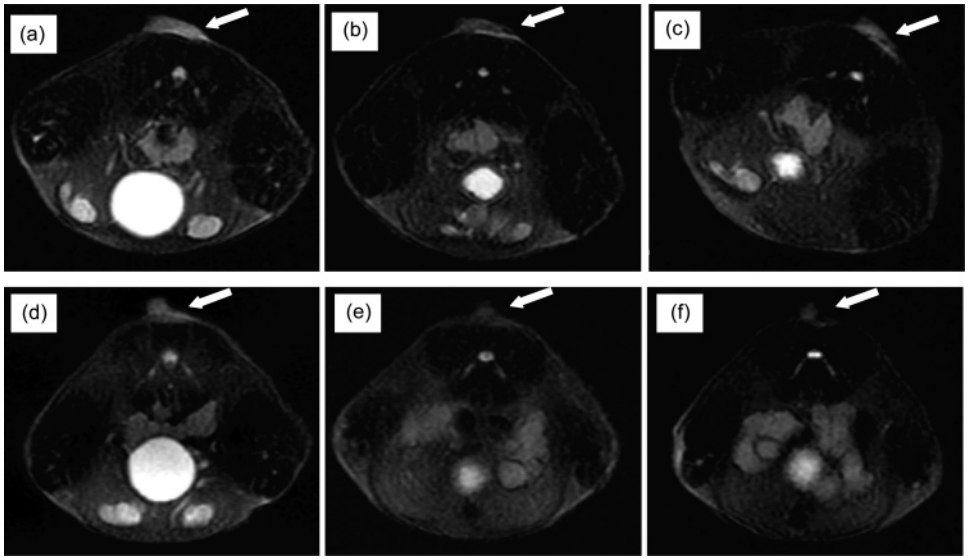

Figure 8. T2-weighted fast-spin−echo images (TR/TE of 4200 ms/102 ms) taken at 0, 1, and 4 h postinjection of 15 mg/kg of IS-SPION (a, b, and c) and 13 mg/kg of SW-SPION (d, e, and f) at the level of the tumor on the back of mice. T2-weighted images (b and e) at 1 h postinjection of SPION show a marked signal drop at the tumor areas compared with those of 0 h (a and d). The arrows denote xenograft tumors.

of the presence or accumulation of iron oxide within the tumor areas. In good agreement with the above in vivo MRI images, larger amounts of iron oxide were observed in the case of SW-SPION than that of IS-SPION. Both in vivo MRI and tissue staining results clearly confirm that the poly(TMSMA-*r*-PEGMA)@SPION could successfully target the tumor tissue via EPR effects through leaky vasculature and thus result in the efficient diagnosis of cancer.

Conclusion

In conclusion, we have presented the fabrication of novel antifouling poly(TMSMA-*r*-PEGMA)@SPION and examined the feasibility of the nanoprobe as an MR contrast agent in vivo as well as in vitro. The poly(TMSMA-*r*-PEGMA)@SPION could detect tumors in vivo using clinical MRI and can be used as a potentially efficient cancer diagnostic probe.[3,56,57] Although the poly(TMSMA-*r*-PEGMA)@SPION did not possess any targeting ligands on their surface,[4,32,33,58] they could diagnose cancer in vivo by directly entering tumor tissues via the EPR effect presumably due to their high stability in plasma as well as the resistance to uptake by the RES. We anticipate that the targeting efficacy of the magnetic nanoprobes developed herein may be significantly increased by attaching targeting ligands on the modified surface.

Acknowledgment. This study was supported by a Grant from the National R&D Program for Cancer Control, Ministry of Health and Welfare, Republic of Korea (0520080-1).

Supporting Information Available: Synthetic procedure of the poly(TMSMA-*r*-PEGMA), FT-IR spectra, TGA graph, powder X-ray diffraction (XRD) patterns of IS-SPION and SW-SPION, and photographs of IS-SPION and SW-SPION dispersed in distilled water at various pHs. This material is available free of charge via the Internet at http://pubs.acs.org.

JA061529K

(49) Weissleder, R.; Stark, D. D.; Engelstad, B. L.; Bacon, B. R.; Compton, C. C.; White, D. L.; Jacobs, P.; Lewis, J. *AJR, Am. J. Roentgenol.* **1989**, *152*, 167−173.
(50) Iannone, A.; Magin, R. L.; Walczak, T.; Federico, M.; Swartz, H. M.; Tomasi, A.; Vannini, V. *Magn. Reson. Med.* **1991**, *22*, 435−442.
(51) Peira, E.; Marzola, P.; Podio, V.; Aime, S.; Sbarbati, A.; Gasco, M. R. *J. Drug Targeting* **2003**, *11*, 19−24.
(52) Magnitsky, S.; Watson, D. J.; Walton, R. M.; Pickup, S.; Bulte, J. W.; Wolfe, J. H.; Poptani, H. *NeuroImage* **2005**, *26*, 744−754.
(53) Weber, R.; Wegener, S.; Ramos-Cabrer, P.; Wiedermann, D.; Hoehn, M. *Magn. Reson. Med.* **2005**, *54*, 59−66.
(54) Ittrich, H.; Lange, C.; Dahnke, H.; Zander, A. R.; Adam, G.; Nolte-Ernsting, C. *RoeFo, Fortschr. Geb. Roentgenstr. Nuklearmed.* **2005**, *177*, 1151−1163.
(55) Pons, H. A.; Soyano, A.; Romano, E. *Immunopharmacology* **1992**, *23*, 29−35.
(56) Weissleder, R. *Nat. Rev. Cancer* **2002**, *2*, 11−18.
(57) Gillies, R. J.; Raghunand, N.; Karczmar, G. S.; Bhujwalla, Z. M. *J. Magn. Reson. Imaging* **2002**, *16*, 430−450.
(58) Suwa, T.; Ozawa, S.; Ueda, M.; Ando, N.; Kitajima, M. *Int. J. Cancer* **1998**, *75*, 626−634.